

# Identification of buried landmines using electromagnetic induction spectroscopy: evaluation of a blind test against ground truth

Haoping Huang<sup>\*a</sup>, Bill San Filippo<sup>b</sup>, Steve Norton<sup>c</sup>, and I. J. Won<sup>d</sup>  
<sup>a,b,c,d</sup> Geophex, Ltd. 605 Mercury Street, Raleigh, NC 27603-2343

## ABSTRACT

The Geophex GEM-3 sensor was tested at a government test site comprised of 980 1-m squares containing buried landmines and clutter (metallic debris). Electromagnetic (EM) induction spectroscopy (EMIS) was used to interpret the data in an attempt to discriminate between the landmines and clutter items. Receiver-operator characteristics (ROC) were constructed based on the results of the analysis. Approximately 92% of the landmines were correctly identified as such, with a false alarm rate of 12%. In this report, we present a comparison of our identification results against the ground truth recently released.

The EMIS method works well for high-metal mines for which the misfit threshold can be easily established, yielding a correct declaration in all cases without false alarms. For medium-metal mines, even though the misfit differences between the mines and clutter are not as clear as those for the high-metal mines, these mines were still identified at very low false alarm rates with the GEM-3 sensor. The low-metal mines may be discriminated from clutter if they yield reliable signals, but often at a much higher false alarm rate. The primary reason for this is that the EM signals from the low-metal mines are intrinsically weak and thus more subject to distortion by noise.

There are several possibilities for improving the low-metal mine identification, including (1) increasing the upper limit of the frequency band to obtain a stronger signal and better defined spectra; (2) decreasing the size of the sensing head to further localize the region of sensitivity of the sensor; (3) displaying the spectral curves and performing the identification in real time to allow operator inspection of the spectral match; and (4) defining a generalized misfit that incorporates signal amplitude and possibly other spectral features such as the quadrature peak.

**Keyword:** Electromagnetic induction spectroscopy, landmine identification, blind test, evaluation

## 1. INTRODUCTION

Most metal detectors can detect metallic landmines, but cannot effectively discriminate a landmine from clutter, which gives rise to high false alarm rates in a cluttered environment. False alarms are anomalies caused by other metallic objects, soil heterogeneities, and other natural and cultural features. False alarms result in unnecessary excavations and significantly contribute to the cost of landmine clearance. A major research objective, therefore, is to develop discrimination (target identification) capabilities.

Many researchers have studied on the problem, e. g., [1-6]. One approach is the electromagnetic induction spectroscopy (EMIS) which is based on the spectral response over a broad induction bandwidth [4-6]. The EMIS response of a metal object depends on its conductivity, magnetic permeability, shape, size, orientation, and depth. Combinations of these factors may sometimes yield similar spectral responses for different targets. Even though the spectral response may not be unique for a target, the method can significantly reduce the number of false alarms and reject clutter. Huang and Won [6] described a normalized EMIS method for identifying targets, which was used to process the data collected at a government test site in early 2001. The Army constructed the so-called ROC (receiver-operator characteristics) curves based on the results, which show overall about 92% of the landmines identified at a false alarm rate of 12%.

Recently, the Army released the ground truth for this site. In this paper, we compare our identification results against the ground truth in an effort to find new ways to improve the sensor and the identification process in the future.

## 2. ELECTROMAGNETIC INDUCTION SPECTROSCOPY

The current EMI landmine detectors cannot distinguish one metallic object from another, so the number of false targets generally far exceeds that of real targets. However, by measuring the broadband spectrum of the secondary field, we obtain a distinct spectral signature that may identify the object. Based on the spectrum, we can “fingerprint” the object. This is the basic concept of EMIS [6].

A general approach for identifying a landmine, as well as for discriminating between landmines and clutter, is to match the EMIS spectrum measured above a target against spectra from known mines that are stored in a library. In a simple scenario, we first conduct a detection survey using multiple frequencies optimally chosen for a given geologic and cultural environment. Once a target is suspected (using audible tone, for instance), we place the sensor directly over the target (a spot of highest tonal output) and record the target’s spectrum. This spectrum is then scanned through a spectral library seeking a match to identify the target as a particular landmine or, if no match is found, to declare it as clutter.

The EMI spectral response of an object is a function of its electrical conductivity, magnetic permeability, shape, size, depth, and orientation. For a specific landmine, however, its shape, size, conductivity, and permeability are given, and the orientation is assumed vertical, leaving depth as the only variable with which the spectral response may vary. Fortunately, in practice the metal parts of a landmine are small compared to the size of, or distance to, the sensor, so the source field at the parts may be considered uniform. Large mines or large clutter items may often be recognized from the audible tone. In the latter case, the sensor can be raised to a proper height to make the primary field uniform at the target. With a uniformly incident field, the mine should produce the same spectral shape regardless of its distance to the sensor. To match the spectral shape independently of amplitude, we normalize an EMIS spectrum by setting, for example, its highest in-phase value to one; in this way, the normalized EMIS spectra measured at various depths will be equal.

Once a library of spectral responses for known landmines is established, a measured spectrum can be scanned through the library to find the best match. Depending on the goodness of fit, we may declare the object as a particular landmine or reject the object as clutter. The declaration requires establishing a match threshold, perhaps for each mine separately, based on experiments. The criterion should be conservative so that the decision process, when uncertain, sides with declaring an object as a mine rather than as clutter. Absolute amplitude of the response is an important indicator for the mine size and depth, which is ignored in the spectral matching process. Thus, even when an observed spectrum matches well in shape with a library spectrum, the object may be declared clutter if the measured amplitude is inconsistent with the expected amplitude within an assumed depth range.

## 3. Demonstration at a US Army Test Site

The test site consists of a blind test grid and a calibration grid. The blind test grid is 49 meters by 20 meters and contains 980 1-m squares. The grid is divided into 20 separate lanes labeled A-T, each with 49 squares labeled 1-49. At the center of each square is buried a mine, a clutter item or nothing (a “blank”).

The calibration grid is 25 meters by 5 meters, separated into five one-meter wide lanes labeled A-E. Known landmines and clutter items are buried in these grid squares. The calibration lanes are used to provide reference signatures prior to testing in the blind test grid. Table 1 lists the types of landmines buried in the blind test grid.

We carried out a demonstration survey using the GEM-3 in early 2001 [6], [7]. The EM data were collected at 10 frequencies ranging from 750 Hz to 23,970 Hz. The EMIS library was first made from the mines seeded in the calibration lanes, and then the EM data were collected over the blind test grid. In the blind grid survey, we duplicated the data collection using two operators equipped with different GEM-3 sensors, in order to check the potential dependence on the sensor or the operator technique.

Table 2 shows the number of mines declared by each sensor (labeled as Sensor 6 and Sensor 7), indicating a remarkable consistency in performance between the two sensors. Based on our test results from the blind test grids, the Army constructed the receiver-operator characteristics (ROC) curves, as shown in Figure 1. The horizontal axis indicates the probability of false alarm (Pfa) and the vertical axis is the probability of detection (Pd). The results from the two GEM-3

sensors are virtually the same, although the data have been collected and processed independently. The inflection point on the ROC curves indicates that, overall, we identified about 92% of the landmines at a false alarm rate of 12%.

#### **4. ANALYSIS OF IDENTIFICATION RESULTS AGAINST GROUND TRUTH**

Even though most of buried landmines were identified and the Pfa may seem acceptably small in this blind test, many more clutter items were declared as low-metal mines. We are currently investigating a number of hardware and algorithmic issues that should help us improve the low-metal performance. Recently, the ground truth at this site was released and we evaluated the identification results from the EM data obtained by one of the sensors.

Table 3 lists the landmines and clutter items buried in the blind test squares and Table 4 summarizes the results of our identification. In total, 101 mines and 440 clutter items were buried in the blind test grids, and 439 squares were blank (empty). There are three types of clutter items, ferrous, nonferrous and radar (nonmetal items). Overall, we correctly identified 93 out of 101 buried mines, misidentified 1 medium-metal and 2 low-metal mines, and missed 5 low-metal mines. For convenience, we group below the buried mines into three categories based on their metal content and examine our declarations for each group.

The first group is the high-metal mines including A and B. Eight items matched to the former and fourteen to the latter. Figure 2 shows the misfit sorted from low to high against the locations where the black bar stands for the mine being declared as the correct mine, and white bars for a clutter item declared as clutter. All buried mines in this group were correctly identified by their names. For these high-metal mines, there is a distinct difference in misfit between the mines and clutter, which allows us to distinguish between the mines and clutter confidently.

Figure 3 depicts the misfit for mines C and D that were grouped as medium-metal mines. Thirty-eight items matched to mine C and thirty-five to mine D. The white bar with black dots stands for a clutter item being misidentified as a mine, and the gray bar with white dots for the mine misidentified as clutter. As can be seen, we declared one C as clutter because the misfit threshold used to declare a target as clutter was mistakenly set too low (It should be 12.3%, but we took 7.3% by accident. Please see [6] page 649). If the threshold were set correctly, all mines C would be identified correctly with one false alarm. The misfits for the items matched to mine D did not show any significant gap, and all of them were identified as mine D with five false alarms. We could have declared the items at squares A6, G33, M40 and M43 as clutter items depending upon their low amplitudes. However, it is difficult to use the lower amplitude limit since deeply buried mines can also cause low amplitudes. If the amplitude is significantly higher than that in the library, we can declare the item as clutter confidently.

The last group is the low-metal mines including E, F, G, H, I, J and K. For this set of mines, if the two or three best misfits were very close together, we claimed more than one name for the mine. As shown in Figure 4, it is often difficult to discriminate the low-metal mines from the clutter items based on their misfits because there is frequently no significant difference between the mines and clutter misfits. Many clutter items were declared correctly as clutter mainly based on their amplitudes being significantly wrong within an assumed depth range. From Tables 3 and 4 we declared 45 out of 52 low-metal mines with 112 false alarms, and misidentified 3 low-metal mines.

One of 20 mines E (H12) was declared as a clutter because the spectrum showed a nonferrous object. The rest were identified as low-metal mines, 18 of them with the correct name. Five mines F were declared as F by name with high confidence due to the lower misfits. However, there are 49 false alarms for mine F, as shown in Table 4, which is ten times higher than the number of real mines. Five mines G were declared as low-metal mines, three with the right name and two with the wrong name.

Regarding the low-metal antitank mines, I and K were all declared mines, and most of them with the correct name. The number of false alarms for these two mines is less than that of the real mines. We declared three mines H and two mines J as blank since the signal levels were lower than noise level. We correctly declared only one H, which was the shallowest (1.06 inch) among the five buried mines H.

There are 42 seeded nonmetal clutter items for radar testing. We declared 40 of them as blank and 2 as clutter items (metal). Also, some blank squares were declared as clutter items and one as a low metal mine, where an audible signal

was definitely received. This is probably because of some non-seeded metal clutter. In total, there were 398 metal clutter items buried, 116 of which we declared as low-metal mines, 222 as clutter, and the remaining 60 as blank.

## 5. IMPROVEMENT OF THE IDENTIFICATION PROCESS

The EMIS method works well for the high-metal mines, in which case the misfit threshold can be easily determined. In practice, one may expect to identify these mines at very low false alarm rates. For medium-metal mines, misfit differences between the mines and clutter items are not as clear as those for the high-metal mines, although we had good success in separating the mine C from clutter and correctly identifying them. The low-metal mines may be discriminated from clutter items if they yield reliable signals, but at much higher false alarm rates. An important future objective will be to reduce the false alarm rate for the low-metal mines.

Our approach is to err on the safe side to prevent a landmine from being classified as clutter. A mine must be declared if both the measured spectrum and amplitude match, for a given threshold, to one of the mines in the library. This may still cause frequent false alarms for low-metal mines. This is primarily due to very weak signals from the low-metal mine, which creates noisy spectra that may match clutter. To improve our discrimination of the low-metal mines, there are several areas worth investigating in addition to improving the sensor's noise performance. One is to increase the upper limit of the frequency band to obtain stronger signals and better-defined spectrum. A second is to decrease the size of the sensing head to confine localization of the field. This may help in reducing the possibility of signal contamination due to small clutter that may intrude into the region of sensitivity, and increase the spatial resolution. The addition of a display device to the sensor may benefit the decision process by allowing an operator to examine the spectral matching visually in real time. Finally, improved discrimination may be possible using more advanced matching algorithms that employ other spectral features.

Since these tests were conducted, we have doubled the frequency band with the upper limit now 48 kHz. Although this only adds one data point on the spectra plotted in logarithmic space, the spectra may be better defined, and yield a better identification. For example, Figure 5a shows spectra of a ferrous clutter item, and the best matched mine (G). We classified this item as a mine G based on its misfit of 10.9%, which is very low for this mine. However, the measured in-phase components are deviating from those in the library as the frequency increases. If one more data point were available at 40 kHz, a higher misfit would result, increasing the chance of a correct declaration of clutter. A future hardware objective is to extend the upper limit of the frequency band to 96 kHz. This should further enhance the detection and discriminating power of the sensor.

The sensing head of the GEM-3 used for this test was 40 cm in diameter. A 30 cm sensing head is under development and test. An even smaller sensing head may have additional advantages. Also, an iPac palm PC has been fitted to the sensor so that the spectral comparison is visible graphically and numerically in real time. This will help an operator to make a decision. For example, one can conclude immediately that the spectra in Figure 5a do not match by visually examining the spectra, but this is not as clear from the value of misfit.

The misfit describes only the sum of absolute differences between the measured and stored spectra, and may miss other features, for example, negative in-phase, position of the quadrature peak, or crossing point of the in-phase and quadrature components. These features can be very useful in declaring clutter items. Figure 5b presents spectra of a clutter object and the best matched mine (I) with a misfit of 17.6%, which results in a declaration of the mine. However, a shift in position of the quadrature peak for the spectra indicates that they do not match. Also, negative in-phase data indicate a ferrous target, and this feature is easy to incorporate into the matching procedure. We declared 8 clutter items as the ferrous mine G. If the sign of the in-phase data were included in the algorithm, four of them could be identified as clutter. Therefore, it may be worth examining a new generalized misfit that includes additional features of this kind.

Some low-metal antitank (AT) mines, such as mine H, may be particularly hard to detect because they are typically buried deeper than antipersonnel (AP) mines. As a means of detecting such mines, we have proposed a new method using the existing GEM-3 sensor [8]. Soil magnetic susceptibility is almost always greater than zero and is detectable using an EM induction sensor such as the GEM-3. When a mine H is buried in soil, it produces a cavity in magnetic susceptibility, which may be detected as a region of low apparent susceptibility compared to the surrounding area. Figure 6 shows an anomaly of the apparent magnetic susceptibility for three squares (D6, D8, and E21) in the calibration grid.

Squares D6 and D8 contain the mine H at depths of 1.25 inch (3.2 cm) and 2.5 inch (6.4 cm), while square E21 contains an irregular stone at a depth of 2 inch (5.1 cm). The landmines produce a susceptibility anomaly of 50% and 42%, which are easy to recognize, while the stone produces no anomaly. In practice, we may detect such a mine from its susceptibility anomaly, and possibly identify it based on the width of the anomaly. For example, mines H were buried at the centers of D2 and L6 in the blind grid at depths of 2.63 inch (6.7 cm) and 1.5 inch (3.8 cm), respectively. We declared the mine at D2 as a blank, because signals from its metal parts were undetectable, and that at L6 as clutter. However, as shown in Figure 7, we can definitely see the anomalies of the apparent susceptibility, which are derived from the in-phase data. The half-widths of the anomalies are 29 cm for D2 and 35 cm for L6, which are close to the size of the mine H (33 cm × 33 cm).

## 6. CONCLUSIONS

A blind test using GEM-3 sensors was performed at a US Army test site, and the EMIS method was used to interpret the EM data, in an attempt to discriminate the landmines from clutter items. ROC curves were built based on the results of the analysis and approximately 92% of the landmines were correctly identified at a false alarm rate of 12%. Analysis of the results against the ground truth indicates that 93 out of 101 seeded mines were correctly identified (most of them by name), misidentified 3 mines as clutter items, and claimed 116 metal clutter items and 1 blank as mines. 56% of the seeded metal clutter items were correctly identified as clutter. We missed 5 low-metal mines because no recognized signals were received.

Our analysis suggests a number of ways of reducing the low-metal false alarm rate. This includes: (1) increasing the upper limit of the frequency band to obtain stronger signals and better defined spectra; (2) decreasing the size of the sensing head to further localize the sensor's region of sensitivity; (3) displaying the spectral curves and performing the identification in real time to allow operator inspection of the spectral match; and finally (4) defining a generalized misfit that explicitly incorporates amplitude data and perhaps additional spectral features.

## ACKNOWLEDGMENT

This work has been supported by the U.S. Army Night Vision Electronic Sensor Directorate (NVESD), Fort Belvoir, Virginia.

## REFERENCES

1. A. H. Trang, P. V. Czipott, and D. A. Waldron, "Characterization of small metallic objects and anti-personnel mines," in *Proc. SPIE*, Orlando, FL, 1997.
2. M. Ozdemir, E. L. Miller, and S. J. Norton, "Localization and characterization of buried objects from multi-frequency, array inductive data," in *Proc. SPIE*, Orlando, FL, 1998.
3. P. Gao, L. Collins, P. M. Garber, N. Geng, and L. Carin, "Classification of landmine-like metal targets using wideband electromagnetic induction", *IEEE Transactions on Geoscience and Remote Sensing*, **38**, no. 3, 1352-1361, 2000.
4. I. J. Won, D. A. Keiswetter, and E. Novikova, "Electromagnetic induction spectroscopy," *Journal of Environmental and Engineering Geophysics*, **3**, No. 1, 27-40, 1998.
5. I. J. Won, D. A. Keiswetter, and T. H. Bell, "Electromagnetic induction spectroscopy for clearing landmines," *IEEE Trans. Geoscience and Remote Sensing*, **39**, No. 4, 703-709, 2001
6. Huang, H., and Won, I. J., "Automated identification of landmines using normalized electromagnetic induction spectroscopy," *IEEE Geoscience and Remote Sensing*, **41**, No.3, 640-651, 2003

7. I. J. Won, D. A. Keiswetter, D. Hanson, E. Novikova, and T. Hall, "GEM-3: A monostatic broadband electromagnetic induction sensor", *Journal of Environmental and Engineering Geophysics*, **2**, No. 1, 53-64, 1997.
8. H. Huang, I. J. Won and B. SanFilipo, "Detecting buried non-metal objects using soil magnetic susceptibility measurements," in Russell S. Harmon, John H. Holloway, Jr., J. T. Broach, Eds., *Detection and Remediation Technologies for Mines and Minelike Targets VIII: Proceedings of SPIE*, **5089**, 1181-1188, 2003.

Table 1. Landmines buried in the blind grids at the test site.

Type	Metal Content	Burial Depth
A (AP)	High	Surface-2 inches
B (AT)	High	1-5 inches
C (AP)	Medium	Surface-2 inches
D (AP)	Medium	Surface-2 inches
E (AP)	Low	Surface-2 inches
F (AP)	Low	Surface-2 inches
G (AP)	Low	Surface-2 inches
H (AT)	Low	1-5 inches
I (AT)	Low	1-5 inches
J (AT)	Low	1-5 inches
K (AT)	Low	1-5 inches

Table 2. Comparison in target declaration statistics of two GEM-3 sensors that were used independently by different operators at. LM: low metal mines.

Type	Quantity Declared	
	Sensor 6	Sensor 7
A	5	5
B	3	3
C	10	10
D	35	35
Other LM Mines	157	159
Clutter or blank	769	768

Table 3. Landmines buried in blind test grid.

Type	Number	Depth (in)	Comments
A	5	0.5-1.75	
B	3	0.94-2.56	
C	11	0.75-2.25	
D	30	0-2.5	
E	20	0-2.88	Some modified
F	5	1-1.5	
G	5	1-2	Some without spring
H	5	1.06-3.5	All Live
I	7	1.44-2.75	All Live except for one
J	5	1.38-4.75	All Live
K	5	1.56-2.56	All Live
Ferrous	353	<b>Total</b>	<b>980</b>
Non ferrous	45	Mine	<b>101</b>
Radar	42	Clutter	<b>440</b>
Blank	439	Blank	<b>439</b>

Table 4. Identification results.

Type	Identified	False alarms	Misidentified	Missed
A	5	0	0	0
B	3	0	0	0
C	10	0	1	0
D	30	5	0	0
E	19	44	1	0
F	5	49	0	0
G	5	8	0	0
H	1	4	1	3
I	7	4	0	0
J	3	0	0	2
K	5	3	0	0
<b>Total</b>	<b>93</b>	<b>117</b>	<b>3</b>	<b>5</b>
Clutter	249			
Blank	521			
<b>Total</b>	<b>770</b>			

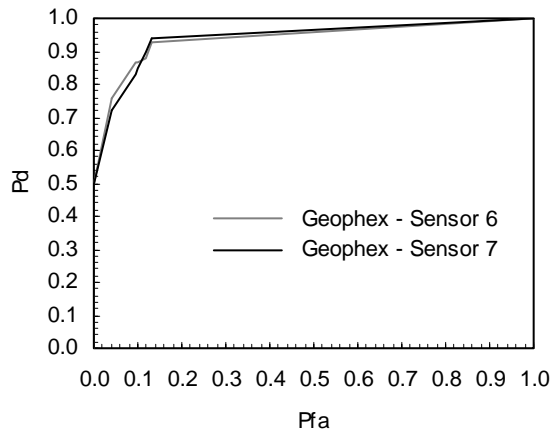


Fig. 1. ROC curves for two GEM-3 sensors showing their performance in terms of the probability of detection (Pd) and probability of false alarms (Pfa) based on the test result from US Army Test Site.

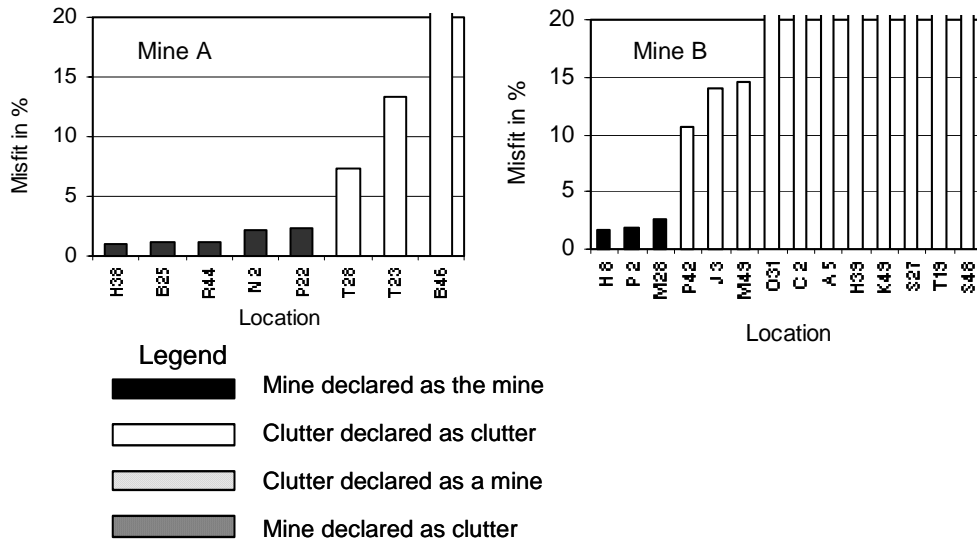


Fig. 2. The misfit against the locations for high-metal mines, A and B. The legend is also for Figures 3 and 4.

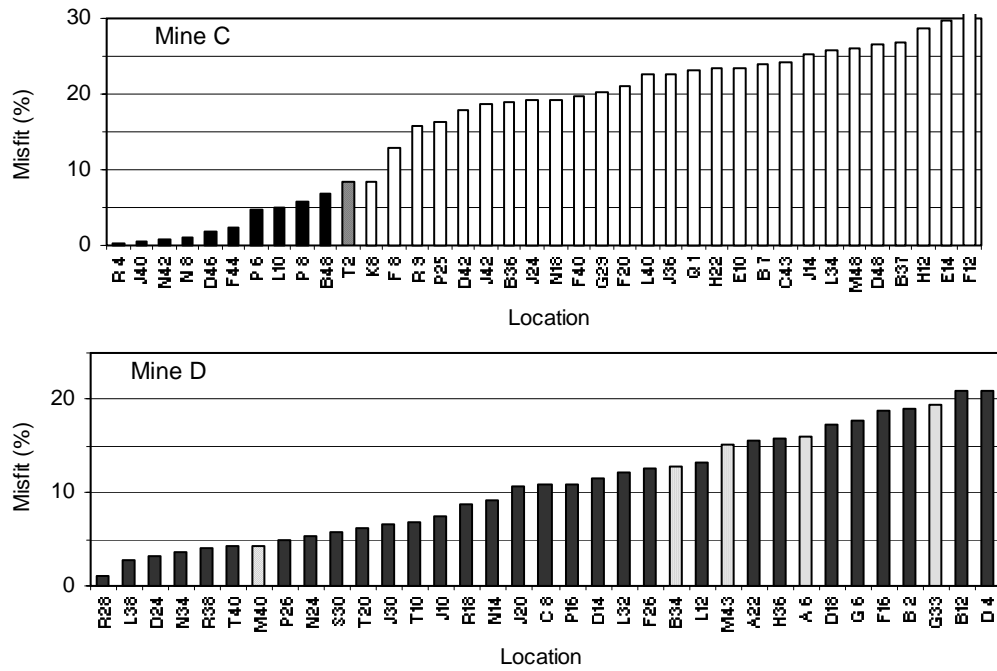


Fig. 3. The misfit against the locations for medium-metal mines, C and D. See Figure 2 for legend.

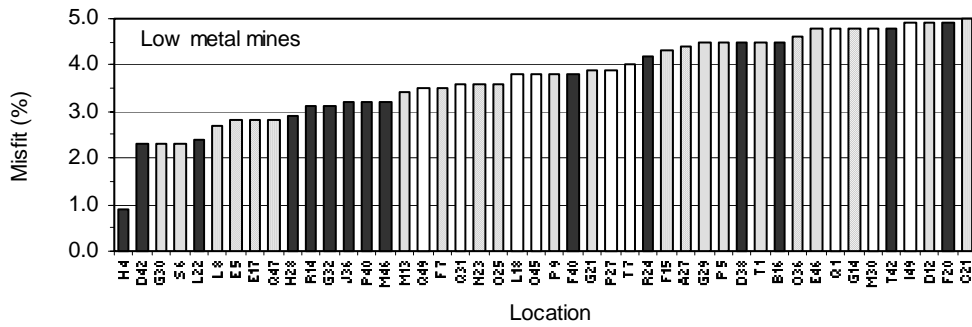


Fig. 4. The misfit against the locations for low-metal mines including E, F, G, H, I, J and K. Note only the misfits less than 5% are shown here as an example. See Figure 2 for legend.

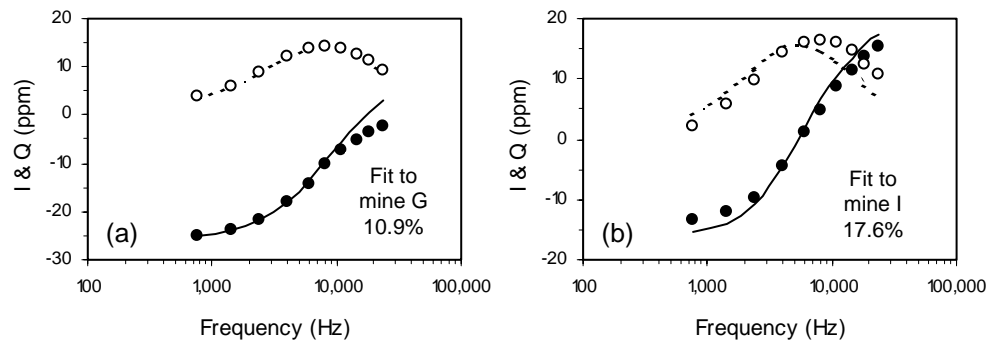


Fig. 5. The normalized EMIS spectra (circles) of clutter objects, along with the best-matched library landmine spectra (lines). Solid line and circles stand for the in-phase component and dashed line and open circles for the quadrature component. (a) Fit to mine G and (b) to mine I.

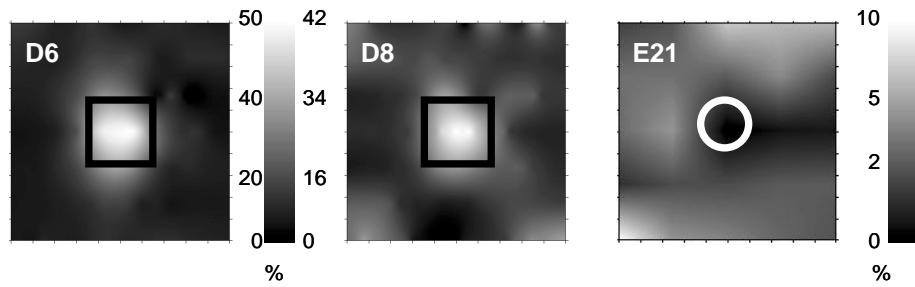


Fig. 6. The apparent susceptibility images at three squares (1 by 1 m) in the calibration grid. Antitank mines H were buried in D6 and D8, and an irregular stone was buried in E21. The squares and circle present roughly the size of the targets.

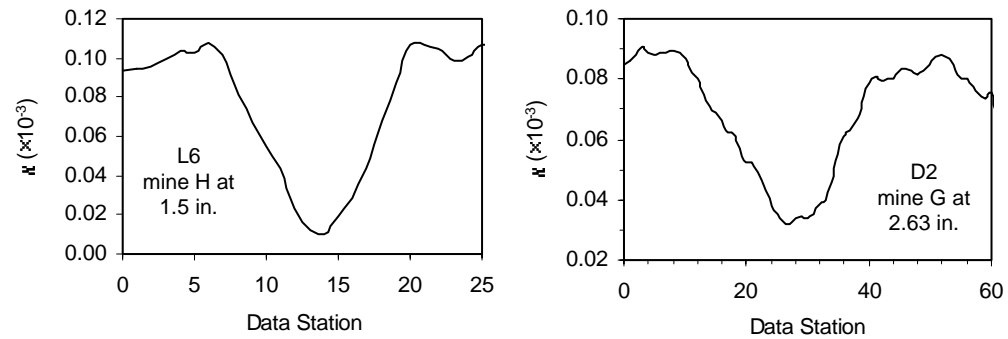


Fig. 7. The apparent susceptibility anomalies observed at D2 and L6 in the blind test grids, where mines H were buried at depths of 6.7 cm and 3.8 cm. The length of profile is 1.4 m.